2020 American Control Conference
Denver, CO, USA, July 1-3, 2020

Global Trajectory Tracking for a Quadrotor through Event-Triggered Control: Synthesis, Simulations, and Experiments*

ZHU Xuan-Zhi[1], Pedro Casau[2] and Carlos Silvestre[3]

Abstract— **This paper presents an event-triggered controller that solves the problem of trajectory tracking for an aerial vehicle with a thrust actuation in a single body-fixed direction and full angular velocity actuation. Under the framework of hybrid dynamical systems, we first design a globally stabilizing hybrid control law and then derive an appropriate event-triggering mechanism for sampling of actuation signals. We prove that bounded reference trajectories are rendered globally asymptotically stable for the closed-loop system. To enable practical implementation of the proposed event-triggered controller on digital platforms, we provide a modified event-triggering mechanism that achieves practical stability while avoiding Zeno solutions. The results are illustrated by numerical simulations and further verified by experiments.**

I. INTRODUCTION

In recent decades, motion control of small aerial vehicles, especially quadrotors, has seen emerging techniques in an attempt to fully exploit their high maneuverability. Among different motion control tasks, trajectory tracking problem is a fundamental one, for which there exist a variety of strategies, including: proportional-integral-derivative (PID) feedback [1], feedback linearization [2], sliding-mode control [3], integral backstepping [4], and adaptive control [5], to name a few. Digital implementation of these controllers requires sufficiently fast periodic sampling of both measurement signals and actuation signals in order to preserve the stability of the closed-loop system. However, the requirement of a sufficiently small sampling period may not be satisfied in some circumstances, such as: limited communication bandwidth for signal transmission, transmission delay, and low computational power for operating the controllers. Besides, it can lead to redundant samples at instants that are not actually needed to achieve the desired stability property.

The advent of event-triggered control allows less frequent sampling while guaranteeing desired levels of performance of the closed-loop system, see [6] and [7] for early approaches. Various Lyapunov-based event-triggering mechanisms have been proposed for the stabilization of continuous-time nonlinear plants. The work in [8]–[10] relies on the existence of an input-to-state (ISS) Lyapunov function. The work in [11] removes the ISS requirement by just focusing on stabilizing the plant state. Event-triggered controllers are feasible only if it can be shown that there exists a positive lower bound to the inter-event time. This has been achieved either by temporal regulation [12]–[14] or by turning off the sampling events near the set to be stabilized [15].

In the context of the trajectory tracking problem of underactuated vehicles, several results achieve position and/or attitude stabilization by event-triggered control. The work in [16] presents an event-triggered feedback law for the trajectory tracking control of a planar vehicle with practical stability and provide sufficient conditions for the absence of Zeno solutions, i.e. those having infinite jumps within finite flow time. The papers [17] and [18] present the design of an event-triggered quaternion-based controller that locally asymptotically stabilize a quadrotor around a desirable fixed attitude while avoiding Zeno solutions, utilizing the results for nonlinear systems affine in the control [19]. The event-triggered PID controller proposed in [20] drives a quadrotor to a fixed position under the assumption that a lower bound for the sampling interval is available. However, control parameters have to be selected carefully to guarantee stability of the system due to the discretization of measured states and the local linearization representation of the orientation, i.e. Euler-angles. The aforementioned works promise local results only, therefore limiting the possibility for inverted flight as one of the aggressive maneuvers. In fact, there exists the inherited topological obstruction to continuous global stabilization of rotational motion [21]. In light of this restriction, we employ hybrid feedback proposed in [22] that helps achieve global asymptotic stability, which results in what is referred to as a *hybrid controller*.

In this paper, we depart from existing strategies by providing a full description of the controller design for global asymptotic trajectory tracking of a quadrotor vehicle. The main contributions are (i) proposing a synthesized control strategy for trajectory tracking of a quadrotor vehicle by combining a globally stabilizing *hybrid controller* and an event-triggering mechanism; (ii) presenting both simulation and experimental results to demonstrate the performance of the proposed control law, where the globally asymptotically stabilizing property is tested with both upright flight mode and inverted flight mode; (iii) excluding Zeno solutions to enable digital implementation of the proposed controller. The remainder of the paper is organized as follows. Math preliminaries are presented in Section II. A dynamical model for the quadrotor and the control objective are introduced in Section III. Section IV focuses on the design of a trajectory tracking controller, followed by simulation results in Section V and experimental results in Section VI. Section VII summaries

*This work was partially supported by the projects MYRG2018-00198-FST and MYRG2016-00097-FST of the University of Macau; by the Macau Science and Technology, Development Fund under Grant FDCT/026/2017/A1 and by Fundação para a Ciência e a Tecnologia (FCT) through Project UID/EEA/50009/2019, and LOTUS PTDC/EEI-AUT/5048/2014 and grant CEECIND/04652/2017.

[1]ZHU Xuan-Zhi is with the Institute for Systems and Robotics, Instituto Superior Técnico, Universidade de Lisboa, Lisboa, Portugal. Email: xuanzhi.zhu@tecnico.ulisboa.pt.

[2]P. Casau is with the Department of Electrical and Computer Engineering at Instituto Superior Técnico, Universidade de Lisboa, Lisboa, Portugal. E-mail address: pcasau@isr.tecnico.ulisboa.pt.

[3]C. Silvestre is with the Department of Electrical and Computer Engineering, Faculty of Science and Technology, University of Macau, Taipa, Macau, on leave from Instituto Superior Técnico, Universidade de Lisboa, Lisboa, Portugal. Email: csilvestre@um.edu.mo.

this paper.

II. PRELIMINARIES

Let $\mathbb{R}_{\geq 0} := [0, \infty[$, $\mathbb{R}_{>0} :=]0, \infty[$, $\mathbb{Z}_{\geq 0} := \{0, 1, 2, \dots\}$, $\mathbb{Z}_{>0} := \{1, 2, \dots\}$. The Euclidean n-space is denoted by $\mathbb{R}^n$, wherein the inner product $\langle \mathbf{x}, \mathbf{y} \rangle := \mathbf{x}^\top \mathbf{y}$ for each $\mathbf{x}, \mathbf{y} \in \mathbb{R}^n$ and the Euclidean norm $|\mathbf{x}| := \sqrt{\langle \mathbf{x}, \mathbf{x} \rangle}$ for each $\mathbf{x} \in \mathbb{R}^n$. In $\mathbb{R}^n$, the unit vector whose i-th component is 1 and the vector whose all entries equal to 0 are denoted as $\mathbf{e}_i$ and $\mathbf{0}$, respectively. Matrices in $\mathbb{R}^{m \times n}$ are represented by regular uppercase characters. In $\mathbb{R}^{n \times n}$, the identity matrix and the matrix whose all entries are equal to 0 are denoted as I_n and 0_n, respectively. The distance of a vector $\mathbf{x} \in \mathbb{R}^n$ to a set $\mathcal{A} \subset \mathbb{R}^n$ is denoted by $|\mathbf{x}|_{\mathcal{A}} := \inf \{|\mathbf{x} - \mathbf{y}| : \mathbf{y} \in \mathcal{A}\}$. The unit open ball centered at the origin is denoted as $\mathbb{B} := \{\mathbf{x} \in \mathbb{R}^n : |\mathbf{x}| < 1\}$. The unit n-sphere centered at the origin is denoted as $\mathbb{S}^n := \{\mathbf{x} \in \mathbb{R}^{n+1} : |\mathbf{x}| = 1\}$.

We make use of the definitions of: a hybrid system; a solution to a hybrid system; stability of a closed set for a hybrid system; and attractivity of a closed set for a hybrid system. These concepts are formalized in [23]. The following definition is made to capture consecutive jumps.

Definition 1: Given a set-valued mapping $\mathcal{G} : \mathbb{R}^n \rightrightarrows \mathbb{R}^n$ and a set $\mathcal{D} \subset \mathbb{R}^n$, we define $\mathcal{G}^1 := \mathcal{G}$ and $\mathcal{G}^{k+1}(\mathbf{x}) := \mathcal{G}\left(\mathcal{D} \cap \mathcal{G}^k(\mathbf{x})\right)$ for each $\mathbf{x} \in \mathbb{R}^n$ and for each $k \in \mathbb{Z}_{>0}$.

The following lemma deals with joint behavior of two set-valued mappings that evolve concurrently.

Lemma 1: Given two set-valued mappings $\mathcal{M}_1 : \mathbb{R}^n \rightrightarrows \mathbb{R}^n$ and $\mathcal{M}_2 : \mathbb{R}^n \rightrightarrows \mathbb{R}^n$, and two sets $\mathcal{A}_1, \mathcal{A}_2 \subset \mathbb{R}^n$ that are closed relative to $\mathbb{R}^n$, if $\mathcal{M}_1$ is outer semicontinuous (locally bounded) relative to $\mathcal{A}_1$ and $\mathcal{M}_2$ is outer semicontinuous (locally bounded) relative to $\mathcal{A}_2$, then the set-valued mapping $\mathcal{M} : \mathbb{R}^n \rightrightarrows \mathbb{R}^n$, given by

$$\mathcal{M}(\mathbf{x}) := \begin{cases} \mathcal{M}_1(\mathbf{x}) & \text{if} \quad \mathbf{x} \in \mathcal{A}_1 \backslash \mathcal{A}_2, \\ \mathcal{M}_2(\mathbf{x}) & \text{if} \quad \mathbf{x} \in \mathcal{A}_2 \backslash \mathcal{A}_1, \\ \mathcal{M}_1(\mathbf{x}) \cup \mathcal{M}_2(\mathbf{x}) & \text{if} \quad \mathbf{x} \in \mathcal{A}_1 \cap \mathcal{A}_2, \end{cases}$$

is outer semicontinuous (locally bounded) relative to $\mathcal{A}_1 \cup \mathcal{A}_2$.

Proof: Outer semicontinuity is preserved due to closedness of the graph of $\mathcal{M}$ relative to $(\mathcal{A}_1 \cup \mathcal{A}_2) \times \mathbb{R}^n$. Local boundedness of $\mathcal{M}$ trivially follows. ∎

The following lemma provides a sufficient condition for the absence of Zeno solutions to a class of hybrid dynamical system.

Lemma 2: Suppose that a hybrid system $\mathcal{H} := (\mathcal{F}, \mathcal{C}, \mathcal{G}, \mathcal{D})$ in $\mathbb{R}^n$ meets the hybrid basic conditions [23, Assumption 6.5] and there exists some $K \in \mathbb{Z}_{>0}$ such that $\mathcal{G}^K(\mathcal{D}) \cap \mathcal{D} = \emptyset$, where $\mathcal{G}^K$ is defined in Definition 1. Then each precompact solution ϕ to $\mathcal{H}$ is not Zeno.

Proof: See the proof of [24, Lemma 2.7] and apply the same argument therein for each $\mathcal{G}^k$ with $k \in \{1, 2, \dots, K\}$. ∎

III. PROBLEM STATEMENT

Consider a fixed orthonormal inertial frame $\{\mathcal{I}\}$ and an orthonormal body-fixed frame $\{\mathcal{B}\}$ that is attached to the center of mass of the vehicle. We follow the formulation in [25] of the kinematics and dynamics of the rigid body vehicle given by

$$\dot{\mathbf{p}} = \mathbf{v}, \quad \dot{\mathbf{v}} = -\frac{1}{m} RT\mathbf{e}_3 + g\mathbf{e}_3, \quad \dot{R} = RS(\boldsymbol{\omega}), \tag{1}$$

where $(\mathbf{p}, \mathbf{v}) \in \mathbb{R}^6$ represents the position and the linear velocity of the vehicle in $\{\mathcal{I}\}$, respectively, $R \in \mathsf{SO}(3) := \left\{R \in \mathbb{R}^{3\times 3} : R^\top R = I_3, \det(R) = 1\right\}$ represents the rotation matrix that maps vectors in $\{\mathcal{B}\}$ to $\{\mathcal{I}\}$, the mapping S is such that $S(\mathbf{a})\mathbf{b} := \mathbf{a} \times \mathbf{b}$ for each $\mathbf{a}, \mathbf{b} \in \mathbb{R}^3$ with $\times$ denoting the cross product, $\boldsymbol{\omega} \in \mathbb{R}^3$ represents the angular velocity of the vehicle in $\{\mathcal{B}\}$, $m \in \mathbb{R}_{>0}$ represents the mass of the vehicle, $T \in \mathbb{R}$ represents the thrust, $g \in \mathbb{R}_{>0}$ represents the local gravitational acceleration. By the second equation of (1), we define $\boldsymbol{\lambda} := R\mathbf{e}_3 \in \mathbb{S}^2$ for each $R \in \mathsf{SO}(3)$, which aligns with the thrust direction in $\{\mathcal{I}\}$. Manipulation of (1) gives rise to the following set of differential equations:

$$\dot{\mathbf{p}} = \mathbf{v}, \quad \dot{\mathbf{v}} = -\frac{1}{m}\boldsymbol{\lambda} T + g\mathbf{e}_3, \quad \dot{\boldsymbol{\lambda}} = -S(\boldsymbol{\lambda})\breve{\boldsymbol{\omega}}, \tag{2}$$

where and $\breve{\boldsymbol{\omega}} := R\boldsymbol{\omega}$ defines the angular velocity of the vehicle in $\{\mathcal{I}\}$.

A reference trajectory is a precompact solution $t \mapsto \mathbf{r}(t) := (\mathbf{p}_d(t), \dot{\mathbf{p}}_d(t), \ddot{\mathbf{p}}_d(t))$ for each $t \in \mathbb{R}_{\geq 0}$ to the differential inclusion $\dot{\mathbf{r}} \in \mathcal{F}_d(\mathbf{r}) := \left\{\mathbf{f}_d\left(\mathbf{r}, \mathbf{p}_d^{(3)}\right) : \mathbf{p}_d^{(3)} \in r\overline{\mathbb{B}}\right\}$, where $r \in \mathbb{R}_{>0}$ and $\mathbf{f}_d\left(\mathbf{r}, \mathbf{p}_d^{(3)}\right) := \left(\dot{\mathbf{p}}_d, \ddot{\mathbf{p}}_d, \mathbf{p}_d^{(3)}\right)$ for each $\left(\mathbf{r}, \mathbf{p}_d^{(3)}\right) \in \mathbb{R}^6 \times r\overline{\mathbb{B}}$, therefore $\operatorname{rge}\mathbf{r} \subset \mathcal{S}_d$ for some compact set $\mathcal{S}_d \subset \mathbb{R}^9$, and the set-valued mapping $\mathcal{F}_d(\mathbf{r})$ satisfies[1]

$$\mathcal{F}_d(\mathbf{r}) \cap \mathcal{T}_{\mathcal{S}_d}(\mathbf{r}) \neq \emptyset \tag{3}$$

for each $\mathbf{r} \in \mathcal{S}_d$, where $\mathcal{T}_{\mathcal{S}_d}(\mathbf{r})$ is the tangent cone to the set $\mathcal{S}_d$ at $\mathbf{r} \in \mathbb{R}^9$, see [23, Definition 5.12]. Such observation is crucial in proving completeness of maximal solutions to a hybrid system. Moreover, we make the following assumption in order to impose continuity of control laws.

Assumption 1: The set $\mathcal{S}_d$ satisfies $\sup_{\mathbf{r} \in \mathcal{S}_d} |\ddot{\mathbf{p}}_d| < g$.

With the definitions above, we present the problem statement as follows.

Problem 1: To design an event-triggered controller that globally asymptotically stabilizes a reference trajectory satisfying Assumption 1 for the dynamical system (2).

IV. CONTROLLER DESIGN

A. Global asymptotic stabilization of both the position and the linear velocity dynamics

First, we design a feedback control law for both the position and the linear velocity error system given a reference trajectory $\mathbf{r} = (\mathbf{p}_d, \dot{\mathbf{p}}_d, \ddot{\mathbf{p}}_d)$. We define the position error and the linear velocity tracking error as

$$\mathbf{z}_1 := \mathbf{p} - \mathbf{p}_d,$$
$$\mathbf{z}_2 := \mathbf{v} - \dot{\mathbf{p}}_d,$$

whose time derivatives are given by

$$\dot{\mathbf{z}}_1 = \mathbf{z}_2, \tag{4a}$$

$$\dot{\mathbf{z}}_2 = -\frac{1}{m}\boldsymbol{\lambda} T + g\mathbf{e}_3 - \ddot{\mathbf{p}}_d, \tag{4b}$$

[1]Equation (3) follows from [23, Lemma 5.26] by continuity of $\mathbf{f}_d$, compactness and convexity of $r\overline{\mathbb{B}}$, implying outer semicontinuity and local boundedness of $\mathcal{F}_d$ relative to $\mathcal{S}_d$.

which can be regarded as a system driven by the *virtual input* $\boldsymbol{\lambda}T$. Let $\mathbf{z} := (\mathbf{z}_1, \mathbf{z}_2)$ and

$$\boldsymbol{\mu}(\mathbf{r}, \mathbf{z}) := \boldsymbol{\beta}(\boldsymbol{\kappa}(\mathbf{z})) + g\mathbf{e}_3 - \ddot{\mathbf{p}}_d$$

for each $(\mathbf{r}, \mathbf{z}) \in \mathcal{S}_d \times \mathbb{R}^6$, where $\boldsymbol{\kappa}(\mathbf{z}) := k_{\mathbf{p}}\mathbf{z}_1 + k_{\mathbf{v}}\mathbf{z}_2$ for each $\mathbf{z} \in \mathbb{R}^6$ with $k_{\mathbf{p}}, k_{\mathbf{v}} \in \mathbb{R}_{>0}$, and the saturation function $\boldsymbol{\beta} : \mathbb{R}^3 \to \mathbb{R}^3$ is such that $\boldsymbol{\beta}(\boldsymbol{\xi}) := (\beta_1(\xi_1), \beta_2(\xi_2), \beta_3(\xi_3))$ for each $\boldsymbol{\xi} := (\xi_1, \xi_2, \xi_3) \in \mathbb{R}^3$, with $\beta_i : \mathbb{R} \to \mathbb{R}$ continuously differentiable and verifying

$$0 < \nabla\beta_i(\xi) \leq M_{\beta_i} \quad \text{for each} \quad \xi \in \mathbb{R}, \tag{5a}$$

$$\beta_i(0) = 0, \tag{5b}$$

$$\lim_{\xi \to \pm\infty} \beta_i(\xi) = \pm K_{\beta_i} \tag{5c}$$

for some $M_{\boldsymbol{\beta}} := (M_{\beta_1}, M_{\beta_2}, M_{\beta_3})$, $K_{\boldsymbol{\beta}} := (K_{\beta_1}, K_{\beta_2}, K_{\beta_3}) \in \mathbb{R}_{>0} \times \mathbb{R}_{>0} \times \mathbb{R}_{>0}$ and for each $i \in \{1, 2, 3\}$.

Lemma 3: Suppose Assumption 1 holds, if

$$|K_{\boldsymbol{\beta}}| < g - \sup_{\mathbf{r} \in \mathcal{S}_d} |\ddot{\mathbf{p}}_d|, \tag{6}$$

then for each $(\mathbf{r}, \mathbf{z}) \in \mathcal{S}_d \times \mathbb{R}^6$, $|\boldsymbol{\mu}(\mathbf{r}, \mathbf{z})| > 0$.

Proof: Using the triangular inequality, the conclusion follows from the properties of the saturation function $\boldsymbol{\beta}$. ■

Suppose the inequality (6) holds onwards, then it is eligible to define the desired direction $\boldsymbol{\lambda}_d$

$$\boldsymbol{\lambda}_d(\mathbf{r}, \mathbf{z}) := \frac{\boldsymbol{\mu}(\mathbf{r}, \mathbf{z})}{|\boldsymbol{\mu}(\mathbf{r}, \mathbf{z})|} \tag{7}$$

for each $(\mathbf{r}, \mathbf{z}) \in \mathcal{S}_d \times \mathbb{R}^6$ and a feedback control law for the thrust T as

$$T(\mathbf{r}, \mathbf{z}, \boldsymbol{\lambda}) := m\boldsymbol{\lambda}^\top \boldsymbol{\mu}(\mathbf{r}, \mathbf{z}) \tag{8}$$

for each $(\mathbf{r}, \mathbf{z}, \boldsymbol{\lambda}) \in \mathcal{S}_d \times \mathbb{R}^6 \times \mathbb{S}^2$.

By assigning the functions defined in (7) and (8) to the *virtual input* in (4b), i.e. $\boldsymbol{\lambda}T = \boldsymbol{\lambda}_d(\mathbf{r}, \mathbf{z})T(\mathbf{r}, \mathbf{z}, \boldsymbol{\lambda}_d(\mathbf{r}, \mathbf{z}))$, we obtain the following closed-loop system

$$\dot{\mathbf{z}}_1 = \mathbf{z}_2, \tag{9a}$$

$$\dot{\mathbf{z}}_2 = -\boldsymbol{\beta}(\boldsymbol{\kappa}(\mathbf{z})). \tag{9b}$$

The following Lemma concerning the stability of the system (9) resembles [26, Lemma 1] but is reproduced to make this paper self-contained.

Lemma 4: The origin of (9) is globally asymptotically stable.

Proof: The unique equilibrium point for the system (9) is the origin $\mathbf{z} = \mathbf{0}$. We choose a Lyapunov function candidate $\overline{V} : \mathbb{R}^6 \to \mathbb{R}$, given by

$$\overline{V}(\mathbf{z}) := \sum_{i=1}^{3} \left(\frac{1}{2} \begin{bmatrix} \beta_i(\kappa_i(\mathbf{z})) \\ \mathbf{e}_i^\top \mathbf{z}_2 \end{bmatrix}^\top D \begin{bmatrix} \beta_i(\kappa_i(\mathbf{z})) \\ \mathbf{e}_i^\top \mathbf{z}_2 \end{bmatrix} + \int_0^{\kappa_i(\mathbf{z})} \beta_i(\tau) d\tau \right),$$

where $\kappa_i(\mathbf{z}) := \mathbf{e}_i^\top \boldsymbol{\kappa}(\mathbf{z})$ for each $\mathbf{z} \in \mathbb{R}^6$ and for each $i \in \{1, 2, 3\}$, $D := \begin{bmatrix} \frac{k_{\mathbf{v}}}{k_{\mathbf{p}}}\gamma & -\gamma \\ -\gamma & k_{\mathbf{p}} \end{bmatrix}$ with $\gamma \in]0, k_{\mathbf{v}}[$ is positive definite. The resulting time derivative of the Lyapunov function candidate evaluated along the solution to the differential equations (9) is

$$\left\langle \nabla\overline{V}(\mathbf{z}), \begin{bmatrix} \mathbf{z}_2 \\ -\boldsymbol{\beta}(\boldsymbol{\kappa}(\mathbf{z})) \end{bmatrix} \right\rangle =: -\overline{W}(\mathbf{z})$$

for each $\mathbf{z} \in \mathbb{R}^6$, where $\overline{W}(\mathbf{z}) = \sum_{i=1}^{3} \Big((k_{\mathbf{v}} - \gamma)\beta_i(\kappa_i(\mathbf{z}))^2 + \frac{\gamma}{k_{\mathbf{p}}} \nabla\beta_i(\kappa_i(\mathbf{z})) \Big(k_{\mathbf{p}} \mathbf{e}_i^\top \mathbf{z}_2 - k_{\mathbf{v}} \beta_i(\kappa_i(\mathbf{z})) \Big)^2 \Big) \geq 0$ for each $\mathbf{z} \in \mathbb{R}^6$, for which the equality holds if and only if $\mathbf{z} = \mathbf{0}$ due to the choice of γ and by the property (5a).

It follows from [27, Theorem 4.2] that the origin is globally asymptotically stable for the system (9). ■

B. Global asymptotic stabilization of (2) by hybrid feedback

Built upon the controller in Section IV-A, we first develop a feedback control law for the angular velocity and then make it globally asymptotically stabilize the complete dynamics by means of hybrid feedback.

From now on, we take into account the attitude kinematics. The error system consisting of the third equation of (2) and (4), driven by T and $\breve{\boldsymbol{\omega}}$, is written as

$$\begin{bmatrix} \dot{\mathbf{z}} \\ \dot{\boldsymbol{\lambda}} \end{bmatrix} = \begin{bmatrix} \mathbf{z}_2 \\ -\frac{1}{m}\boldsymbol{\lambda}T + g\mathbf{e}_3 - \ddot{\mathbf{p}}_d \\ -S(\boldsymbol{\lambda})\breve{\boldsymbol{\omega}} \end{bmatrix} =: \mathbf{f}(\mathbf{r}, \mathbf{z}, \boldsymbol{\lambda}, T, \breve{\boldsymbol{\omega}}),$$

where the function $\mathbf{f}$ is defined for each $(\mathbf{r}, \mathbf{z}, \boldsymbol{\lambda}, T, \breve{\boldsymbol{\omega}}) \in \mathcal{S}_d \times \mathbb{R}^6 \times \mathbb{S}^2 \times \mathbb{R} \times \mathbb{R}^3$.

For global asymptotic tracking of the reference trajectory, we employ synergistic hybrid feedback [22] to overcome the topological obstruction to global stabilization of rotational motion, $\boldsymbol{\lambda}$ in our case, by continuous state feedback [21]. In this direction, we make use of a logic variable $q \in \mathcal{Q} := \{-1, 1\}$, define $\mathbf{x}_0 := (\mathbf{r}, \mathbf{z}, \boldsymbol{\lambda}, q)$, and choose a new Lyapunov function candidate

$$V_q(\mathbf{r}, \mathbf{z}, \boldsymbol{\lambda}) := \overline{V}(\mathbf{z}) + \epsilon \Big(1 - q\boldsymbol{\lambda}^\top \boldsymbol{\lambda}_d(\mathbf{r}, \mathbf{z}) \Big) \tag{10}$$

that is continuously differentiable on some open set containing the set $\mathcal{S}_{\mathbf{x}_0} := \mathcal{S}_d \times \mathbb{R}^6 \times \mathbb{S}^2 \times \mathcal{Q}$, where $\epsilon \in \mathbb{R}_{>0}$.

Following a backstepping approach, a feedback law for the angular velocity can be chosen as

$$\begin{aligned} \breve{\boldsymbol{\omega}}\left(\mathbf{x}_0, \mathbf{p}_d^{(3)}\right) := {} & \frac{1}{q\epsilon}|\boldsymbol{\mu}(\mathbf{r}, \mathbf{z})| S(\boldsymbol{\lambda}) \begin{bmatrix} 0_3 \\ I_3 \end{bmatrix}^\top \nabla\overline{V}(\mathbf{z}) \\ & + \frac{k_{\boldsymbol{\omega}}}{q} S(\boldsymbol{\lambda}) \boldsymbol{\lambda}_d(\mathbf{r}, \mathbf{z}) + \breve{\boldsymbol{\omega}}_d\left(\mathbf{r}, \mathbf{z}, \boldsymbol{\lambda}, \mathbf{p}_d^{(3)}\right) \end{aligned} \tag{11}$$

for each $\left(\mathbf{x}_0, \mathbf{p}_d^{(3)}\right) \in \mathcal{S}_{\mathbf{x}_0} \times r\overline{\mathbb{B}}$, where $k_{\boldsymbol{\omega}} \in \mathbb{R}_{>0}$, the first term counteracts the position and linear velocity errors, the second term penalizes the deviation of $\boldsymbol{\lambda}$ from $\pm\boldsymbol{\lambda}_d$, the third term represents the desired angular velocity given by $\breve{\boldsymbol{\omega}}_d\left(\mathbf{r}, \mathbf{z}, \boldsymbol{\lambda}, \mathbf{p}_d^{(3)}\right) := \frac{S(\boldsymbol{\lambda}_d(\mathbf{r}, \mathbf{z}))}{|\boldsymbol{\mu}(\mathbf{r}, \mathbf{z})|} \Big(J_{\boldsymbol{\beta}}(\boldsymbol{\kappa}(\mathbf{z})) \Big(k_{\mathbf{p}}\mathbf{z}_2 - k_{\mathbf{v}} \big(\boldsymbol{\beta}(\boldsymbol{\kappa}(\mathbf{z})) + S(\boldsymbol{\lambda})^2 \boldsymbol{\mu}(\mathbf{r}, \mathbf{z}) \big) \Big) - \mathbf{p}_d^{(3)} \Big)$ for each $\left(\mathbf{r}, \mathbf{z}, \boldsymbol{\lambda}, \mathbf{p}_d^{(3)}\right) \in \mathcal{S}_d \times \mathbb{R}^6 \times \mathbb{S}^2 \times r\overline{\mathbb{B}}$, where $J_{\boldsymbol{\beta}}(\boldsymbol{\kappa}(\mathbf{z}))$ is the Jacobian matrix of the saturation function $\boldsymbol{\beta}$ evaluated at $\boldsymbol{\kappa}(\mathbf{z})$.

To represent the closed-loop dynamics driven by the feedback control laws (8) and (11), we define

$$\mathbf{f}_0\left(\mathbf{x}_0, \mathbf{p}_d^{(3)}\right) := \begin{bmatrix} \mathbf{f}_d\left(\mathbf{r}, \mathbf{p}_d^{(3)}\right) \\ \mathbf{f}\left(\mathbf{r}, \mathbf{z}, \boldsymbol{\lambda}, T(\mathbf{r}, \mathbf{z}, \boldsymbol{\lambda}), \breve{\boldsymbol{\omega}}\left(\mathbf{x}_0, \mathbf{p}_d^{(3)}\right)\right) \\ 0 \end{bmatrix} \tag{12}$$

for each $\left(\mathbf{x}_0, \mathbf{p}_d^{(3)}\right) \in \mathcal{S}_{\mathbf{x}_0} \times r\overline{\mathbb{B}}$ such that the time derivative of $\mathbf{x}_0 \mapsto V_q(\mathbf{r}, \mathbf{z}, \boldsymbol{\lambda})$ evaluated along the solution to the differential equation (12) is obtained as

$$\begin{aligned} W(\mathbf{r}, \mathbf{z}, \boldsymbol{\lambda}) &:= \left\langle \nabla V_q(\mathbf{r}, \mathbf{z}, \boldsymbol{\lambda}), \mathbf{f}_0\left(\mathbf{x}_0, \mathbf{p}_d^{(3)}\right)\right\rangle \\ &= -\overline{W}(\mathbf{z}) - \epsilon k_{\boldsymbol{\omega}} \left| S(\boldsymbol{\lambda}) \boldsymbol{\lambda}_d(\mathbf{r}, \mathbf{z}) \right|^2 \end{aligned} \tag{13}$$

for each $(\mathbf{r}, \mathbf{z}, \boldsymbol{\lambda}) \in \mathcal{S}_d \times \mathbb{R}^6 \times \mathbb{S}^2$, which equals zero if and only if $(\mathbf{z}, \boldsymbol{\lambda}) = \left(\mathbf{0}, \pm \frac{g\mathbf{e}_3 - \ddot{\mathbf{p}}_d}{|g\mathbf{e}_3 - \ddot{\mathbf{p}}_d|}\right)$.

For global asymptotic stabilization, we define the the hybrid system $\mathcal{H}_0 := (\mathcal{F}_0, \mathcal{C}_0, \mathcal{G}_0, \mathcal{D}_0)$ given by

$$\mathcal{H}_0 : \begin{cases} \dot{\mathbf{x}}_0 \in \mathcal{F}_0(\mathbf{x}_0) := \left\{ \mathbf{f}_0\left(\mathbf{x}_0, \mathbf{p}_d^{(3)}\right) : \mathbf{p}_d^{(3)} \in r\overline{\mathbb{B}} \right\} \\ \quad \text{if} \quad \mathbf{x}_0 \in \mathcal{C}_0 := \{\mathbf{x}_0 \in \mathcal{S}_{\mathbf{x}_0} : \Delta(\mathbf{x}_0) \leq \eta\}, \\ \mathbf{x}_0^+ \in \mathcal{G}_0(\mathbf{x}_0) := (\mathbf{r}, \mathbf{z}, \boldsymbol{\lambda}, -q) \\ \quad \text{if} \quad \mathbf{x}_0 \in \mathcal{D}_0 := \{\mathbf{x}_0 \in \mathcal{S}_{\mathbf{x}_0} : \Delta(\mathbf{x}_0) \geq \eta\}, \end{cases} \tag{14}$$

where $\operatorname{dom}\mathcal{F}_0 = \operatorname{dom}\mathcal{G}_0 = \mathcal{S}_{\mathbf{x}_0}$, $\Delta(\mathbf{x}_0) := V_q(\mathbf{r}, \mathbf{z}, \boldsymbol{\lambda}) - \min_{\rho \in \mathcal{Q}} V_\rho(\mathbf{r}, \mathbf{z}, \boldsymbol{\lambda})$ for each $\mathbf{x}_0 \in \mathcal{S}_{\mathbf{x}_0}$, and $\eta \in]0, 2\epsilon[$ such that $\{V_q\}_{q \in \mathcal{Q}}$ is synergistic with synergy gap exceeding η, see [22] for detail.

Lemma 5: Suppose Assumption 1 holds, then the set $\mathcal{A}_0 := \left\{\mathbf{x}_0 \in \mathcal{S}_{\mathbf{x}_0} : \mathbf{z} = \mathbf{0}, \boldsymbol{\lambda} = q\frac{g\mathbf{e}_3 - \ddot{\mathbf{p}}_d}{|g\mathbf{e}_3 - \ddot{\mathbf{p}}_d|}\right\}$ is globally asymptotically stable for the hybrid system $\mathcal{H}_0$ defined by (14).

Proof: Due to space constraint, we omit the details but provide a sketch of the proof: $\mathcal{H}_0$ meeting the hybrid basic conditions [23, Assumption 6.5] by the maximum theorem [28, Theorem 9.14]; each maximal solution to $\mathcal{H}_0$ being precompact by [23, Proposition 6.10]; $\mathcal{A}_0$ being globally attractive for $\mathcal{H}_0$ by [23, Corollary 8.4]; stability of $\mathcal{A}_0$ for $\mathcal{H}_0$ by [23, Theorem 3.18]. ∎

C. Event-triggered implementation of the hybrid controller in Section IV-B

Now, we consider the effect of sampling of actuation signals, namely synchronized sampling of both thrust T and the angular velocity $\check{\boldsymbol{\omega}}$, resulting from zero-order-hold devices. We denote the sampled thrust and the sampled angular velocity as s_1 and $\mathbf{s}_2$, respectively. Let $\mathbf{x} := (\mathbf{x}_0, s_1, \mathbf{s}_2)$. To make the control law event-triggered, consider the following the hybrid system $\mathcal{H} := (\mathcal{F}, \mathcal{C}, \mathcal{G}, \mathcal{D})$ given by

$$\mathcal{H} : \begin{cases} \quad \dot{\mathbf{x}} \in \mathcal{F}(\mathbf{x}) := \left\{ \begin{bmatrix} \mathbf{f}_d\left(\mathbf{r}, \mathbf{p}_d^{(3)}\right) \\ \mathbf{f}(\mathbf{r}, \mathbf{z}, \boldsymbol{\lambda}, s_1, \mathbf{s}_2) \\ \mathbf{0} \end{bmatrix} : \mathbf{p}_d^{(3)} \in r\overline{\mathbb{B}} \right\} \\ \quad \text{if} \quad \mathbf{x} \in \mathcal{C} := \mathcal{C}_1 \cap \mathcal{C}_2, \\ \mathbf{x}^+ \in \mathcal{G}(\mathbf{x}) := \mathcal{G}_1(\mathbf{x}) \cup \mathcal{G}_2(\mathbf{x})) \\ \quad \text{if} \quad \mathbf{x} \in \mathcal{D} := \mathcal{D}_1 \cup \mathcal{D}_2, \end{cases} \tag{15}$$

where $\operatorname{dom}\mathcal{F} = \operatorname{dom}\mathcal{G} = \mathcal{S}_{\mathbf{x}} := \mathcal{S}_{\mathbf{x}_0} \times \mathbb{R} \times \mathbb{R}^3$, $\mathcal{C}_1 := \mathcal{C}_0 \times \mathbb{R} \times \mathbb{R}^3$, $\mathcal{D}_1 := \mathcal{D}_0 \times \mathbb{R} \times \mathbb{R}^3$,

$$\mathcal{C}_2 := \left\{ \mathbf{x} \in \mathcal{S}_{\mathbf{x}} : \max_{\mathbf{u} \in \mathcal{F}(\mathbf{x})} \left\langle \nabla \hat{V}_q(\mathbf{x}), \mathbf{u} \right\rangle \leq \sigma \hat{W}(\mathbf{x}) \right\},$$

$$\mathcal{D}_2 := \left\{ \mathbf{x} \in \mathcal{S}_{\mathbf{x}} : \max_{\mathbf{u} \in \mathcal{F}(\mathbf{x})} \left\langle \nabla \hat{V}_q(\mathbf{x}), \mathbf{u} \right\rangle \geq \sigma \hat{W}(\mathbf{x}) \right\},$$

where the function $\mathbf{x} \mapsto \hat{V}_q(\mathbf{x})$ is an extension of the function (10) such that $\hat{V}_q(\mathbf{x}) = V_q(\mathbf{r}, \mathbf{z}, \boldsymbol{\lambda})$ for each $\mathbf{x} \in \mathcal{S}_{\mathbf{x}}$ and is continuously differentiable on some neighborhood of $\mathcal{S}_{\mathbf{x}}$, the function $\mathbf{x} \mapsto \hat{W}(\mathbf{x})$ is an extension of the function (13) such that $\hat{W}(\mathbf{x}) = W(\mathbf{r}, \mathbf{z}, \boldsymbol{\lambda})$ for each $\mathbf{x} \in \mathcal{S}_{\mathbf{x}}$ and is continuously differentiable on some neighborhood of $\mathcal{S}_{\mathbf{x}}$, $\sigma \in]0, 1[$ intended to allow some flow time for sampling,

$$\mathcal{G}_1(\mathbf{x}) := (\mathcal{G}_0(\mathbf{x}_0), s_1, \mathbf{s}_2)$$

triggers a switching event of the logic variable with $\operatorname{dom}\mathcal{G}_1 = \mathcal{D}_1$, and

$$\mathcal{G}_2(\mathbf{x}) := \left\{ \begin{bmatrix} \mathbf{x}_0 \\ T(\mathbf{r}, \mathbf{z}, \boldsymbol{\lambda}) \\ \check{\boldsymbol{\omega}}\left(\mathbf{x}_0, \mathbf{p}_d^{(3)}\right) \end{bmatrix} : \mathbf{p}_d^{(3)} \in r\overline{\mathbb{B}} \right\}$$

triggers a sampling event with $\operatorname{dom}\mathcal{G}_2 = \mathcal{D}_2$.

Theorem 6: Suppose Assumption 1 holds, then the set $\mathcal{A} := \left\{\mathbf{x} \in \mathcal{S}_{\mathbf{x}} : \mathbf{z} = \mathbf{0}, \boldsymbol{\lambda} = q\frac{g\mathbf{e}_3 - \ddot{\mathbf{p}}_d}{|g\mathbf{e}_3 - \ddot{\mathbf{p}}_d|}\right\}$ is globally asymptotically stable for the hybrid system $\mathcal{H}$ defined by (15).

Proof: This proof follows similar lines as the proof of Lemma 5 with some differences: proving that $\mathcal{H}$ meets the hybrid basic conditions uses, in addition, [23, Lemma 5.15], [28, Proposition 9.9], and Lemma 1. ∎

Remark 1: The global convergence of error state $\mathbf{z}$ to the origin corresponds to trajectory tracking, while the global convergence of $\boldsymbol{\lambda}$ corresponds to the fact that the thrust direction tends to align itself with the desired one, which solves the Problem 1.

D. Avoidance of Zeno solutions for the controller in Section IV-C

To have a positive lower bound on the inter-event time, which implies the absence of Zeno behavior of solutions, is essential for practical implementation of our proposed controller on digital platforms, and the following corollary provides a method that ensures absence of Zeno solutions by modifying $\mathcal{H}$. Notice that for the controller in Section IV-B, $\mathcal{G}_0(\mathcal{D}_0) \subset \mathcal{C}_0 \backslash \mathcal{D}_0$, which implies that $\mathcal{G}_0(\mathcal{D}_0) \cap \mathcal{D}_0 = \emptyset$, which implies the existence of some positive lower bound between consecutive jumps for each maximal solution to $\mathcal{H}_0$ by [24, Lemma 2.7]. For the controller in Section IV-C, multiple jumps are possible at the same flow time. In fact, because the nonempty set $\mathcal{G}^k(\mathcal{D}) \cap \mathcal{D} \subset \mathcal{A}$ for each $k \in \{4, 5, \dots\}$ with $\mathcal{G}^k$ given in Definition 1, there exists a complete discrete solution at $\mathcal{A}$, e.g. $\mathbf{x}(0, j+1) = \mathcal{G}_2(\mathbf{x}(0, j))$ such that the solution $\mathbf{x}(0, j) \in \mathcal{A}$ for each $j \in \mathbb{Z}_{\geq 0}$. A straightforward fix for this problem is to remove the possibility of any jumps within an arbitrarily small neighborhood $\mathcal{A}$, as formalized in the following corollary.

Corollary 1: Suppose Assumption 1 holds. Let $\hat{\mathcal{A}} := \left\{\mathbf{x} \in \mathcal{S}_{\mathbf{x}} : \hat{V}_q(\mathbf{x}) \leq \delta\right\}$ with some $\delta \in \mathbb{R}_{>0}$ and consider the hybrid system

$$\hat{\mathcal{H}} := (\mathcal{F}, \hat{\mathcal{C}}_1 \cap \hat{\mathcal{C}}_2, \hat{\mathcal{G}}, \hat{\mathcal{D}}_1 \cup \hat{\mathcal{D}}_2), \tag{16}$$

where $\hat{\mathcal{C}}_1 := \mathcal{C}_1 \cup \hat{\mathcal{A}}$, $\hat{\mathcal{C}}_2 := \mathcal{C}_2 \cup \hat{\mathcal{A}}$, $\hat{\mathcal{D}}_1 := \mathcal{D}_1 \cap \overline{\mathcal{S}_{\mathbf{x}} \backslash \hat{\mathcal{A}}}$, $\hat{\mathcal{D}}_2 := \mathcal{D}_2 \cap \overline{\mathcal{S}_{\mathbf{x}} \backslash \hat{\mathcal{A}}}$, $\hat{\mathcal{G}}(\mathbf{x}) := \mathcal{G}_1(\mathbf{x}) \cup \mathcal{G}_2(\mathbf{x})$, and $\mathcal{F}$, $\mathcal{C}_1$, $\mathcal{C}_2$, $\mathcal{G}_1$, $\mathcal{G}_2$, $\mathcal{D}_1$, and $\mathcal{D}_2$ are given in Section IV-C. Then, the set $\hat{\mathcal{A}}$ is globally asymptotically stable for the hybrid system $\hat{\mathcal{H}}$ and $\hat{\mathcal{H}}$ has no Zeno solutions.

Proof: Proof of global asymptotic stability of the set $\hat{\mathcal{A}}$ for the hybrid system $\hat{\mathcal{H}}$ follows similar lines as in Theorem 6. In particular, $\hat{\mathcal{G}}^3(\hat{\mathcal{D}}_1 \backslash \hat{\mathcal{D}}_2) = \emptyset$, $\hat{\mathcal{G}}^3(\hat{\mathcal{D}}_2 \backslash \hat{\mathcal{D}}_1) = \emptyset$, and $\hat{\mathcal{G}}^3(\hat{\mathcal{D}}_1 \cap \hat{\mathcal{D}}_2) \subset \hat{\mathcal{G}}(\hat{\mathcal{D}}_2 \backslash \hat{\mathcal{D}}_1)$. As a result, $\hat{\mathcal{G}}^3(\hat{\mathcal{D}}) \cap \hat{\mathcal{D}} \subset (\hat{\mathcal{C}} \backslash \hat{\mathcal{D}}) \cap \mathcal{S}_{\mathbf{x}} \backslash \hat{\mathcal{A}} \cap \hat{\mathcal{D}} = \emptyset$. Therefore, $\hat{\mathcal{G}}^k(\hat{\mathcal{D}}) \cap \hat{\mathcal{D}} = \emptyset$ for each $k \in \{3, 4, \dots\}$ and it follows then from Lemma 2 that there exists a positive lower bound between consecutive jumps for each maximal solution to $\hat{\mathcal{H}}$, which implies the absence of Zeno solutions. ■

Remark 2: We notice the trade-off between achieving global asymptotic stabilization and avoidance of Zeno solutions. For practical consideration, we can choose δ arbitrarily small such that practical stability is guaranteed.

V. SIMULATION RESULTS

In order to verify the performance of the proposed control scheme, this section presents simulation results by making use of MATLAB/Simulink software with the hybrid equation solver [29]. A circular trajectory parametrized in flow time is chosen to be the position reference, i.e. $\mathbf{p}_d(t) = \left(\frac{6}{5}\cos(t), \frac{6}{5}\sin(t), -0.5\right)\mathrm{m}$ for each $t \in \mathbb{R}_{\geq 0}$, such that Assumption 1 holds. For each $i \in \{1, 2, 3\}$, the β_i function in (5) is chosen as $\beta_i(\xi) = \frac{2K_{\beta_i}}{\pi} \arctan\left(\frac{\pi M_{\beta_i}}{2K_{\beta_i}}\xi\right)$ for each $\xi \in \mathbb{R}$, where $M_{\beta_i}, K_{\beta_i} \in \mathbb{R}_{>0}$. In each subsequent simulation, the initial states are chosen in $\mathcal{S}_{\mathbf{x}}$ and the hybrid systems are simulated with a hybrid time horizon of 20 seconds and 1500 times. Parameters used in subsequent simulations are $m = 0.2\,\mathrm{kg}$, $g = 9.8\,\mathrm{m\,s^{-2}}$, $k_{\mathbf{p}} = 2$, $k_{\mathbf{v}} = 2$, $\gamma = 0.8$, $k_{\boldsymbol{\omega}} = 5$, $M_{\boldsymbol{\beta}} = (1, 1, 1)$, $K_{\boldsymbol{\beta}} = (1, 1, 1)$, $\epsilon = 20$, $\eta = 36$, $\sigma = 0.01$, and $\delta = 10^{-3}$, such that the inequality (6) holds. The initial state $\mathbf{x}(0,0) \in \mathcal{C} \cap \mathcal{D}_1$, wherein $\mathbf{z}_1(0,0) \approx (4.2835, -0.4902, -0.9571)\,\mathrm{m}$, $\mathbf{z}_2(0,0) \approx (-0.4590, 0.0881, -0.4070)\,\mathrm{m\,s^{-1}}$, $\boldsymbol{\lambda}(0,0) \approx (0.0004, -0.4388, -0.8986)$, $q(0,0) = 1$, $s_1(0,0) = 0\,\mathrm{N}$, $\mathbf{s}_2(0,0) = \mathbf{0}\,\mathrm{s^{-1}}$.

Two possible solutions to the hybrid system $\hat{\mathcal{H}}$ defined in (16) with the same initial state $\mathbf{x}(0,0)$ are shown in Fig. 1 and Fig. 2, denoted by $\mathbf{x}$ and $\mathbf{x}^*$. $\mathbf{x}$ in solid line undergoes one switching for the value of q, i.e. $q(t,j) = -1$ for each $(t,j) \in \mathrm{dom}\,\mathbf{x} \backslash \{(0,0)\}$, while $\mathbf{x}^*$ in dashed line undergoes no switching for the value of q^*, i.e. $q^*(t,j) = 1$ for each $(t,j) \in \mathrm{dom}\,\mathbf{x}^*$. Despite the difference in the time evolution of these two solutions, they both approach the set $\hat{\mathcal{A}}$, with $\mathbf{x}$ converging faster than $\mathbf{x}^*$ due to a smaller initial angular distance with respect to the set $\hat{\mathcal{A}}$. $\mathbf{x}$ represents the case when the vehicle performs trajectory tracking in inverted flight mode, i.e. $s_1(t,j) \leq 0$ for each $(t,j) \in \mathrm{dom}\,\mathbf{x}$. On the contrary, $\mathbf{x}^*$ manifests a thrust direction reversal for the vehicle at $t \approx 0.4\,\mathrm{s}$, witnessed by a surge of $|\mathbf{s}_2^*|$, and eventually achieves trajectory tracking in upright flight mode. It is interesting to note that the proposed controller reacts against increasing error norms by increasing number of jumps, e.g. $t \approx 5\,\mathrm{s}$.

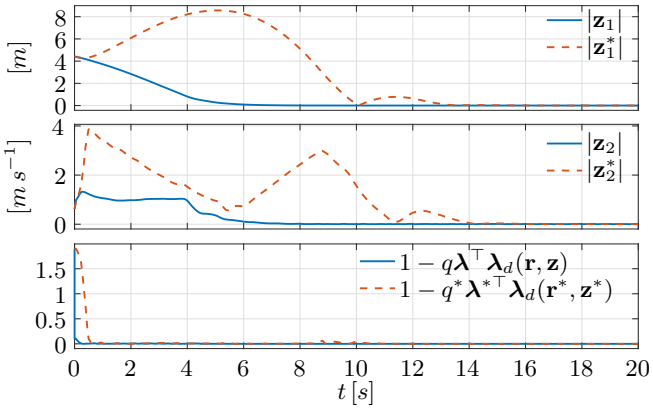

Fig. 1. Time evolution of the norms of position errors, velocity errors, and the angular errors for two possible solutions $\mathbf{x}$ and $\mathbf{x}^*$ to $\hat{\mathcal{H}}$ in (16) with the same initial state $\mathbf{x}(0,0)$.

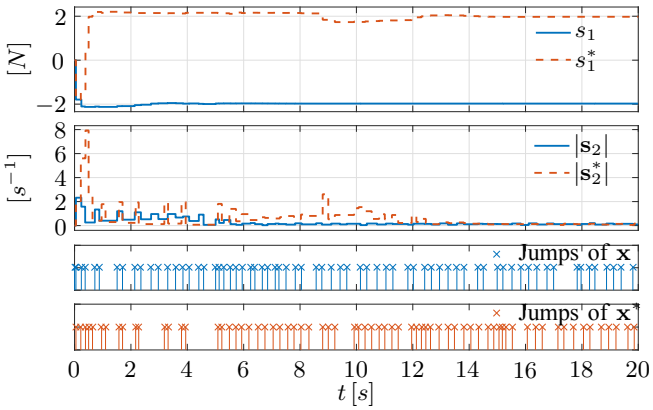

Fig. 2. Time evolution of the sampled thrust, the sampled angular velocity, and the jumps for two possible solutions $\mathbf{x}$ and $\mathbf{x}^*$ to $\hat{\mathcal{H}}$ in (16) with the same initial state $\mathbf{x}(0,0)$.

VI. EXPERIMENTAL RESULTS

The rapid prototyping and testing setup at the SCORE laboratory [30], University of Macau, was used to experimentally validate our control strategy. Experiments were conducted in a MATLAB/Simulink environment that integrated an optical motion capture system [31], and radio communication with the quadrotor. The quadrotor used for the experiments is a radio controlled BLADE 200QX [32]. The vehicle has a flying weight of $0.216\,\mathrm{kg}$ (batteries, radio receiver, and motion capture markers included), and has four brushless motors which drive four propellers located at the end of each arm. The experimental quadrotor lacks on-board sensors and the state of the quadrotor must be estimated resorting to external sensors. To this effect, we placed six motion capture markers with which the position and orientation information can be obtained through the motion capture system. The state measurements from the motion capture system are obtained every $0.01\,\mathrm{s}$ while the actuation signals are sent through the radio frequency transmitter every $0.045\,\mathrm{s}$. We present the experimental results of the most trivial trajectory tracking task, namely to track a fixed-point in space parametrized as $\mathbf{p}_d(t) = (0, 0, -0.5)\,\mathrm{m}$ for each $t \in \mathbb{R}_{\geq 0}$. Other functions and parameters are chosen to be the same as those in Section V except that $m = 0.216\,\mathrm{kg}$, $g = 9.79\,\mathrm{m\,s^{-2}}$, $K_{\boldsymbol{\beta}} = (1, 1, 4.3)$, and $\sigma = 0.9$. We tested the tracking performance of the quadrotor in two scenarios: inverted flight and upright flight. For the former case, we held it inverted above the ground in order: a) not to crash the quadrotor; b) to switch the logic variable q, and release

it at $t = 0\,\mathrm{s}$. For the latter case, we placed the quadrotor on the ground and made the event-triggered controller work from $t = 0\,\mathrm{s}$.

As seen in Fig. 3, the position error $\mathbf{z}_1$ first went through initial transients and then stayed within a neighborhood of zero. Readers may resort to a video clip available online for this experiment [33] .

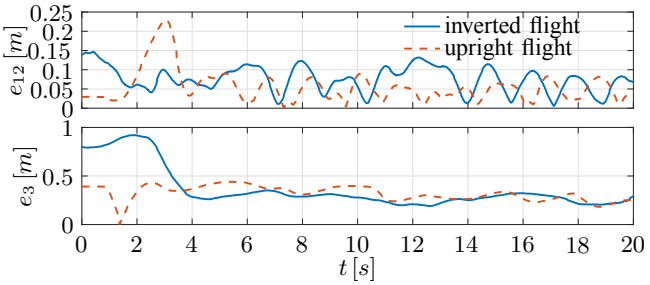

Fig. 3. Comparison of the position tracking performance between inverted flight mode and upright flight mode, where $e_{12} := |(z_{11}, z_{12})|$ and $e_3 := |z_{13}|$ with $(z_{11}, z_{12}, z_{13}) := \mathbf{z}_1$.

VII. CONCLUSION

This paper presented a solution to the problem of trajectory tracking for a class of underactuated quadrotors, taking into consideration the sampling of the actuation signals using zero-order-hold devices. Based on the hybrid dynamical model of the system, an event-triggered control law was devised such that bounded reference trajectories are rendered globally asymptotically stable for the closed-loop hybrid system. For practical consideration, we modified the data of the hybrid system in order to avoid Zeno solutions. Experiments were conducted, validating the performance of our controller.

REFERENCES

[1] G. M. Hoffmann, S. L. Wasl, and C. J. Tomlin, "Quadrotor helicopter trajectory tracking control," in *In Proc. AIAA Guidance, Navigation, and Control Conf*, 2012.

[2] T. J. Koo and S. Sastry, "Output tracking control design of a helicopter model based on approximate linearization," in *Proceedings of the 37th IEEE Conference on Decision and Control (Cat. No.98CH36171)*, vol. 4, 1998, pp. 3635–3640 vol.4.

[3] R. Xu and U. Ozguner, "Sliding mode control of a quadrotor helicopter," in *Proceedings of the 45th IEEE Conference on Decision and Control*, Dec 2006, pp. 4957–4962.

[4] D. Cabecinhas, R. Cunha, and C. Silvestre, "A nonlinear quadrotor trajectory tracking controller with disturbance rejection," *Control Engineering Practice*, vol. 26, pp. 1 – 10, 2014.

[5] Z. T. Dydek, A. M. Annaswamy, and E. Lavretsky, "Adaptive control of quadrotor uavs: A design trade study with flight evaluations," *IEEE Transactions on Control Systems Technology*, vol. 21, no. 4, pp. 1400–1406, July 2013.

[6] K. J. Åström and B. Bernhardsson, "Comparison of periodic and event based sampling for first-order stochastic systems," *IFAC Proceedings Volumes*, vol. 32, no. 2, pp. 5006 – 5011, 1999.

[7] K.-E. Åarzén, "A simple event-based pid controller," *IFAC Proceedings Volumes*, vol. 32, no. 2, pp. 8687 – 8692, 1999.

[8] P. G. Otanez, J. R. Moyne, and D. M. Tilbury, "Using deadbands to reduce communication in networked control systems," in *Proceedings of the 2002 American Control Conference (IEEE Cat. No.CH37301)*, vol. 4, May 2002, pp. 3015–3020 vol.4.

[9] E. Kofman and J. H. Braslavsky, "Level crossing sampling in feedback stabilization under data-rate constraints," in *Proceedings of the 45th IEEE Conference on Decision and Control*, Dec 2006, pp. 4423–4428.

[10] P. Tabuada, "Event-triggered real-time scheduling of stabilizing control tasks," *IEEE Transactions on Automatic Control*, vol. 52, no. 9, pp. 1680–1685, Sept 2007.

[11] A. Seuret, C. Prieur, and N. Marchand, "Stability of non-linear systems by means of event-triggered sampling algorithms," *IMA Journal of Mathematical Control and Information*, vol. 31, no. 3, pp. 415–433, Sept 2014.

[12] M. Abdelrahim, R. Postoyan, J. Daafouz, and D. Nešić, "Stabilization of nonlinear systems using event-triggered output feedback controllers," *IEEE Transactions on Automatic Control*, vol. 61, no. 9, pp. 2682–2687, Sep. 2016.

[13] D. Nešić, A. R. Teel, and D. Carnevale, "Explicit computation of the sampling period in emulation of controllers for nonlinear sampled-data systems," *IEEE Transactions on Automatic Control*, vol. 54, no. 3, pp. 619–624, March 2009.

[14] W. P. M. H. Heemels, J. H. Sandee, and P. P. J. V. D. Bosch, "Analysis of event-driven controllers for linear systems," *International Journal of Control*, vol. 81, no. 4, pp. 571–590, 2008.

[15] R. Postoyan, P. Tabuada, D. Nešić, and A. Anta, "A framework for the event-triggered stabilization of nonlinear systems," *IEEE Transactions on Automatic Control*, vol. 60, no. 4, pp. 982–996, April 2015.

[16] R. Postoyan, M. C. Bragagnolo, E. Galbrun, J. Daafouz, D. Nešić, and E. Castelan, "Nonlinear event-triggered tracking control of a mobile robot: design, analysis and experimental results," in *9th IFAC Symposium on Nonlinear Control Systems, NOLCOS 2013*, Toulouse, France, Sep. 2013, pp. 318–323.

[17] J.-F. Guerrero-Castellanos, J. J. Téllez-Guzmán, S. Durand, N. Marchand, J. Alvarez-Muñoz, and V. R. Gonzalez-Diaz, "Attitude stabilization of a quadrotor by means of event-triggered nonlinear control," *Journal of Intelligent & Robotic Systems*, vol. 73, no. 1-4, pp. 123–135, 2014.

[18] J. F. Guerrero-Castellanos, N. Marchand, S. Durand, A. Vega-Alonzo, and J. J. Téllez-Guzmán, "Event-triggered attitude control for flying robots using an event approach based on the control," in *2015 International Conference on Event-based Control, Communication, and Signal Processing (EBCCSP)*, June 2015, pp. 1–8.

[19] N. Marchand, S. Durand, and J. F. G. Castellanos, "A general formula for event-based stabilization of nonlinear systems," *IEEE Transactions on Automatic Control*, vol. 58, no. 5, pp. 1332–1337, May 2013.

[20] S. Durand, B. Boisseau, N. Marchand, and J. F. Guerrero-Castellanos, "Event-based pid control application to a mini quadrotor helicopter," *Journal of Control Engineering and Applied Informatics*, vol. 20, no. 1, pp. 36–47, 2018.

[21] S. P. Bhat and D. S. Bernstein, "A topological obstruction to continuous global stabilization of rotational motion and the unwinding phenomenon," *Systems & Control Letters*, vol. 39, no. 1, pp. 63 – 70, 2000.

[22] C. G. Mayhew and A. R. Teel, "Synergistic potential functions for hybrid control of rigid-body attitude," in *Proceedings of the 2011 American Control Conference*, June 2011, pp. 875–880.

[23] R. Goebel, R. G. Sanfelice, and A. R. Teel, *Hybrid Dynamical Systems: modeling, stability, and robustness*. Princeton University Press, 2012.

[24] R. G. Sanfelice, R. Goebel, and A. R. Teel, "Invariance principles for hybrid systems with connections to detectability and asymptotic stability," *IEEE Transactions on Automatic Control*, vol. 52, no. 12, pp. 2282–2297, Dec 2007.

[25] J. J. Craig, *Introduction to robotics: mechanics and control*. Pearson/Prentice Hall, 2009.

[26] P. Casau, R. G. Sanfelice, R. Cunha, D. Cabecinhas, and C. Silvestre, "Robust global trajectory tracking for a class of underactuated vehicles," *Automatica*, vol. 58, pp. 90 – 98, 2015.

[27] H. K. Khalil, *Nonlinear systems*. Prentice-Hall, 2002.

[28] R. K. Sundaram, *A First Course in Optimization Theory*. Cambridge University Press, 1996.

[29] R. G. Sanfelice, D. A. Copp, and P. Nanez. (2014) Hybrid equations (hyeq) toolbox v2.02 a toolbox for simulating hybrid systems in matlab/simulink. https://hybrid.soe.ucsc.edu/software/.

[30] Sensor based Cooperative Robotics Research (SCORE) laboratory, at the Department of Electrical and Computer Engineering of the Faculty of Science and Technology, University of Macau. https://score.fst.um.edu.mo/. (2018)

[31] Vicon Motion Systems Ltd. https://www.vicon.com/. (2018)

[32] Horizon Hobby Inc. http://www.bladehelis.com/. (2014)

[33] Event-triggered Control for Trajectory Tracking of a Quadrotor Vehicle. https://youtu.be/eD8iBOllcmU/. (2019)